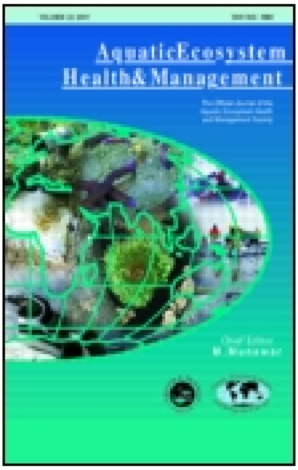

Aquatic Ecosystem Health & Management
Publication details, including instructions for authors and subscription information:
http://www.tandfonline.com/loi/uaem20

Fluctuations of satellite-derived chlorophyll concentrations and optical indices at the Southern Yellow Sea

Qianguo Xing [a b], Hubert Loisel [b], François G. Schmitt [b], David Dessailly [b], Yanju Hao [a], Qiuying Han [a] & Ping Shi [a]

[a] Chinese Academy of Sciences, LCEP, Yantai Institute of Coastal Zone Research, Laishan District, Yantai, 264003, China

[b] Centre National de la Recherche Scientifique (CNRS), Laboratory of Oceanology and Geosciences, UMR 8187 LOG, 62930, Wimereux, France

Version of record first published: 11 Jul 2012

To cite this article: Qianguo Xing, Hubert Loisel, François G. Schmitt, David Dessailly, Yanju Hao, Qiuying Han & Ping Shi (2012): Fluctuations of satellite-derived chlorophyll concentrations and optical indices at the Southern Yellow Sea, Aquatic Ecosystem Health & Management, 15:2, 168-175

To link to this article: http://dx.doi.org/10.1080/14634988.2012.688480

Fluctuations of satellite-derived chlorophyll concentrations and optical indices at the Southern Yellow Sea

Qianguo Xing,[1,2,*] Hubert Loisel,[2] François G. Schmitt,[2] David Dessailly,[2] Yanju Hao,[1] Qiuying Han,[1] and Ping Shi[1]

[1]*Chinese Academy of Sciences, LCEP, Yantai Institute of Coastal Zone Research, Laishan District, Yantai 264003, China*

[2]*Centre National de la Recherche Scientifique (CNRS), Laboratory of Oceanology and Geosciences, UMR 8187 LOG 62930, Wimereux, France*

**Corresponding author: qgxing@yahoo.com*

*Time series of chlorophyll-*a *concentration (chl* a*), backscattering coefficient at 490 nm (*$b_{bp}(490)$*) and spectral slope of* b_{bp} *(*γ*) derived from satellite imagery of ocean color were used to study the aquatic ecosystem of the Southern Yellow Sea during the time period of 1997–2007. Our study indicated that chl* a *increased in offshore waters by 0.02 mg* m^{-3} y^{-1} *(*$p < 0.05$*), in contrast to a decline observed in the middle and low-latitude global waters.* $b_{bp}(490)$*, a proxy of total suspended particulate matter concentration did not have any significant trend, while* γ*, a proxy of the relative proportion of small-sized and larger particles in the surface ocean, decreased significantly. Annual spring phytoplankton blooms occurred in nearshore and offshore waters of the central Southern Yellow Sea; while autumn blooms only occurred in nearshore waters.*

Keywords: Chlorophyll-*a* concentration, particle back-scattering coefficients, particle size distribution

Introduction

Coastal waters are highly impacted by human activities and runoff from land, but difficult to monitor due to the rapidly changing dynamics and the temporal and spatial limitations of traditional sampling. Phytoplankton is a key indicator of aquatic ecosystem status, and the concentration of the pigment chl *a* can be used as a proxy of the abundance of phytoplankton. Remote sensing techniques for monitoring phytoplankton can aid the study of aquatic ecosystems (McClain, 2009).

Phytoplankton is a key component of particulate assemblages in marine waters. The size of algal particles is generally larger than suspended sediments in coastal waters that are usually dominated by finer inorganic particles. The particle size distribution of phytoplankton assemblages varies with the algae species as well as environmental conditions. The abundance of phytoplankton and non-algal particles, and their size distribution influence the inherent optical properties.

Backscattering of light for pure sea water has a strong power law dependence on wavelength, i.e. $b_{bw}(\lambda) \sim \lambda^{-4.32}$. The spectral dependence of the backscattering coefficients of suspended marine particles, b_{bp}, can be approximated as follows, $b_{bp}(\lambda) = C\lambda^{-\gamma}$, where C is proportional to the particle concentration and γ is the exponent of the spectral dependency. Recent field and theoretical studies indicate a trend of an increase in γ with an increase in small-sized particles (Reynolds et al.,

Aquatic Ecosystem Health & Management, 15(2):168–175, 2012. ISSN: 1463-4988 print / 1539-4077 online
DOI: 10.1080/14634988.2012.688480

2001; Wozniak and Stramski, 2004; Loisel et al., 2006; Kostadinov et al., 2007). For large particles, $\gamma \approx 0$, and for small particles, $\gamma > 0$ (Carder et al., 1999). Note negative values can occur, especially in coastal areas, due to the absorption depression effect, particularly in the blue part of the spectrum. Kopelevich (1983) divides particles into two classes depending on their size: large particles which have a strong forward scattering peak and small wavelength dependence, with $\gamma = 0.3$, and small particles which have an almost symmetric scattering function and stronger wavelength dependence, with $\gamma = 1.7$ (Mobley, 1994). As reported by Loisel et al. (2006), γ is generally smaller in eutrophic coastal waters than in oligotrophic waters in the open seas. Based on in situ and satellite estimates, γ, the wavelength dependence of b_{bp}, ranges from 0 to 3 (Loisel et al., 2006).

To date, chl a, $b_{bp}(\lambda)$ and γ can be estimated by satellite (Loisel et al., 2006) and used to evaluate the changes and trend of chlorophyll-a concentrations in marine waters (Vantrepotte et al., 2011). Analyses using the spatial and temporal distribution of chl a, $b_{bp}(\lambda)$ and γ will be helpful to understand the dynamic process of particles in specific waters (e.g. D'Sa et al., 2007), and further to understand its ecosystem dynamics. The purpose of this study is to analyze the spatio-temporal patterns of chl a, $b_{bp}(\lambda)$ and γ of the Southern Yellow Sea over the time period 1997–2007.

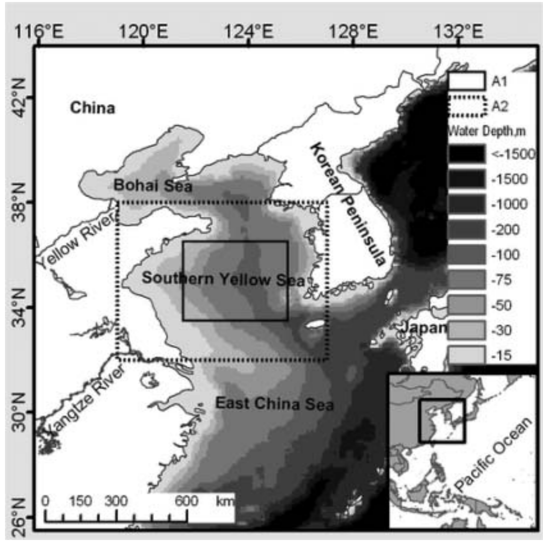

Figure 1. The bathymetry of the Southern Yellow Sea and its vicinities. Area of A1 (121.5E, 36.5N–125.5E, 33.5N) stands for the central SYS, mainly dominated by off-shore waters with the water depth more than 15 m; A2 (119E, 38N–127E, 32N) is a larger area including the nearshore waters; A3 is the area un-overlapped by A1 and A2, A1-(A1∩A2).

Data and methodology

The Yellow Sea (YS) is located between China and the Korean peninsula; it is a marginal sea of the Pacific Ocean. The southern part of Yellow Sea (Southern Yellow Sea [SYS]) is next to the East China Sea. The YS is an important productive region for fisheries, and its coastal zone includes aquaculture, tourism, transportation, and habitat for migrating birds. Its trophic status is significantly impacted by inputs from land and coastal activities such as aquaculture (Liu et al., 2009). The SYS is characterized as Case-II waters for which inherent optical properties not only depend on phytoplankton and associated material, but also other suspended and dissolved material of terrestrial origin. For the purpose of this study the SYS was divided in two different areas, one mainly dominated by offshore waters with water depths higher than 15m, the other by shallow coastal waters (A1 and A3[A2-A1], Figure 1). Previous researchers have tried to investigate differences in the coastal waters and the central SYS (offshore waters) (Fu et al., 2009), but the findings were limited by the temporal-spatial coverage of traditional field investigations. Data for offshore waters are particularly scarce for time series analysis.

The monthly chlorophyll-a concentration (chl a) with a 9×9 km spatial resolution was obtained from the satellite imaging products of Sea-viewing Wide Field-of-view Sensor (SeaWiFS). The data were processed using the OC4-v4 algorithm (O'Reilly et al., 1998). The algorithm is commonly biased in the estimation of chl a for Case-II waters like the SYS (Loisel et al., 2010). However, we have found that our estimates with chl a are not significantly impacted (Li, L. et al., Yantai Institute of Coastal Zone Research, CAS, in prep.). The back-scattering coefficient at 490 nm ($b_{bp}(490)$) and the wavelength dependency (γ) were retrieved from the monthly SeaWiFS water leaving irradiance (Lw) using the methods proposed by Loisel and Stramski (2000) and Loisel et al. (2006), respectively. The concerned time period is from September 1997 to August 2007.

The mean value and standard deviation of each parameter were calculated for all the pixels in regions A1 and A2. The value in A3 (M_{A3}) was calculated on the basis of the mean values of A1 and

A2 (M_{A1} and M_{A2}) as well as the areas of A1 and A2, i.e. $M_{A3} = (A1 \times M_{A1} - A2 \times M_{A2})/(A1\text{-}A2)$.

Annual averages were calculated by averaging the 12 monthly averages. To investigate seasonal variability, monthly averages were calculated for the ten years of the study. The standard deviations were also calculated.

Results

Seasonal changes of chl *a*, $b_{bp}(490)$ and γ

Phytoplankton blooms had different seasonal timing between nearshore and offshore waters. In the nearshore waters, the peaks of chl *a* occur in February and August, and the minimum occured in June (Figure 2a). This observation agrees with previous studies based on field measurements performed in the nearshore waters, e.g. the Jianzhou Bay (Li et al., 2005) and Laizhou Bay (Chen et al., 2001). The lowest chl *a* in the offshore waters were found between June and August, and in contrast to nearshore waters, there was only one peak of phytoplankton abundance occurring in April. The seasonal variability of $b_{bp}(490)$ differed from that of chl *a*. In contrast to chl *a*, the seasonal patterns in b_{bp} did not significantly differ between nearshore and offshore waters. For both regions, $b_{bp}(490)$ was larger during the winter-spring seasons (January–March) and smaller in summer seasons (July and August) (Figure 2b). In offshore waters, the peak of $b_{bp}(490)$ was in March, which is both different to the peak in the nearshore waters in February and to the peak of phytoplankton biomass in April. The wavelength dependency of the particulate backscattering, γ, reached its largest value in winter season (January) and its lowest value by the end of the summer season (August) (Figure 2c). However, the seasonal pattern in γ was very similar for the three defined regions.

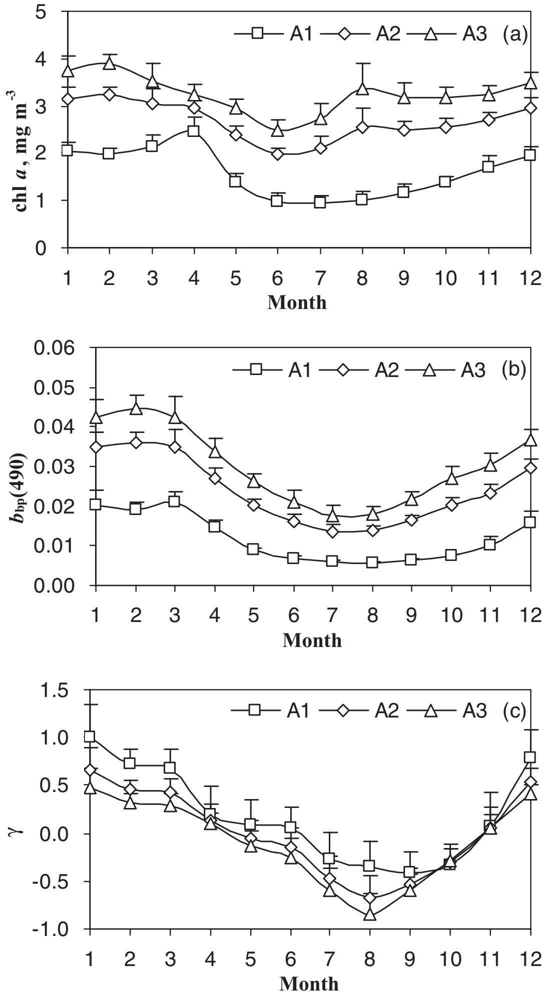

Figure 2. The seasonal variations of (a) chl *a*, (b) $b_{bp}(490)$ and (c) γ in the Southern Yellow Sea and its vicinities. Standard deviations are presented by error bars.

Time series data of chl *a*, $b_{bp}(490)$ and γ

Chl *a*, $b_{bp}(490)$ and γ presented strong annual cycles in both A1 (offshore) and A2 (nearshore) regions (Figure 3). As shown by the data during September 1997 to August 1998, chl *a* in this area was close to a log-normal distribution (Figure 4); The spatially-averaged chl *a* during the time period of 1997 to 2007 was log-normally distributed for A1 while normally distributed for A2 (Figure 5). The absolute values of chl *a* and $b_{bp}(490)$ were always lower in A1 than in A2 where nearshore waters were also included. Due to deposition, particulate concentration (including phytoplankton and non-algal particles) decreased from nearshore to offshore waters. The wavelength dependency of backscattering particles, γ, was higher in offshore waters than in nearshore waters.

Inter-annual variability and contemporary trend

Figure 6 presents the inter-annual variations of chl *a*, $b_{bp}(490)$ and γ from September 1997 to August 2007. Linear regression is used to analyze the trends and the coefficients are listed in Table 1. Chl *a* in the offshore waters of the central SYS

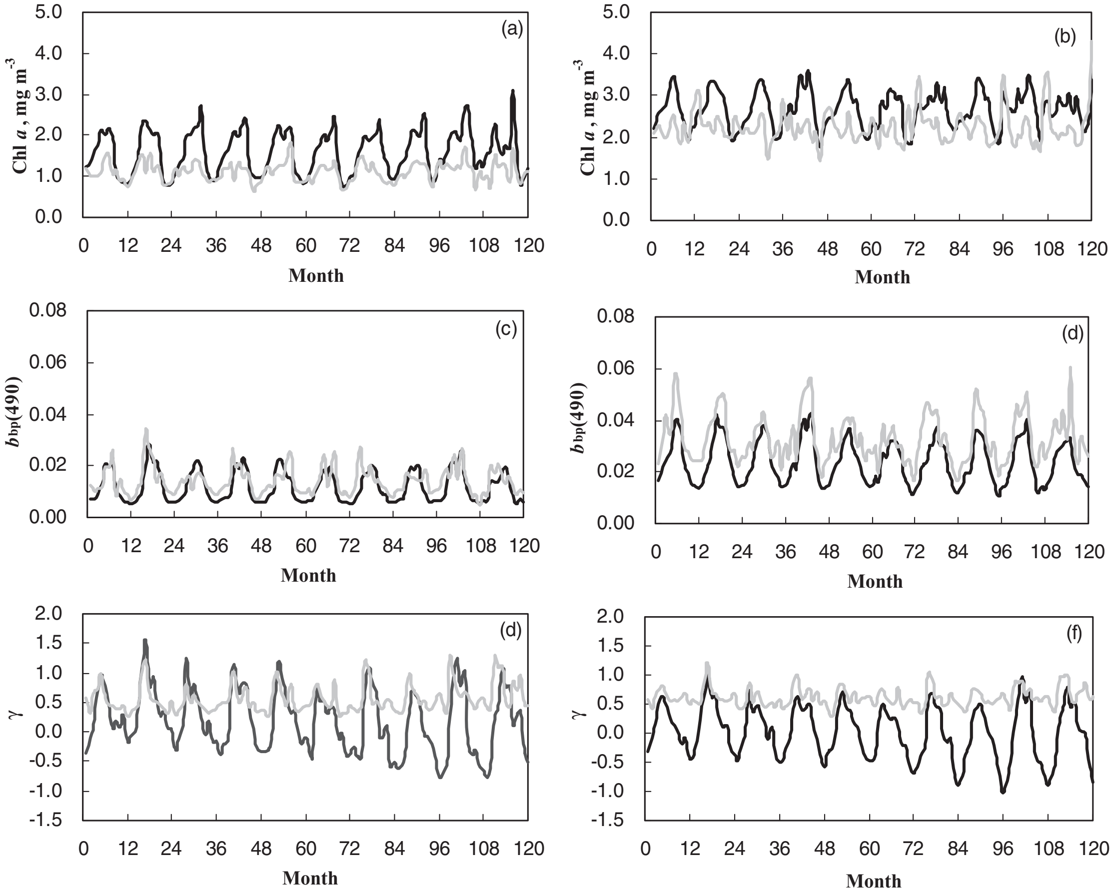

Figure 3. The monthly variations of chl a, $b_{bp}(490)$ and γ during the 1997–2007 time period for the A1 (panels a, c, e) and A2 (b, d, f) regions. The solid line corresponds to monthly-averaged value, and the grey line corresponds to standard deviation.

significantly increased for chl a ($p < 0.05$) over the ten year period at a rate of 0.02 mg m^{-3} y^{-1}, and there was also a significant increase ($p < 0.05$) in the peak value of chl a in the spring bloom (April). In the larger area (A2) or the nearshore waters (A3), this increase was not significant, perhaps due to the high background levels of chl a and stronger fluctuations in the nearshore waters. $b_{bp}(490)$ showed a non-significant declining trend during the 1997–2007 time period both for nearshore waters ($p > 0.05$) and offshore waters ($p > 0.5$). This suggests that although the phytoplankton concentration increased over the ten year period, the concentration of the entire particulate assemblage, as estimated from the remotely sensed particulate backscattering coefficient, did not change significantly over

Table 1. The linear trends of chl a, $b_{bp}(\lambda)$ and γ during 1997–2007.*

	A1			A2			A3		
Y	a	b	p	a	b	p	a	b	p
chl a	0.02	1.4776	0.0415	0.0102	2.6226	0.2891	0.005	3.2266	0.6382
$b_{bp}(490)$	−0.00005	0.0122	0.3478	−0.0002	0.025	0.0785	−0.0003	0.0317	0.0706
γ	−0.0375	0.3926	0.0174	−0.0279	0.1612	0.0092	−0.0228	0.0392	0.0062

*Each trend can be given as $Y = aX + b$, where a and b are coefficients, X is the number of years, p is the p-value in F-test.

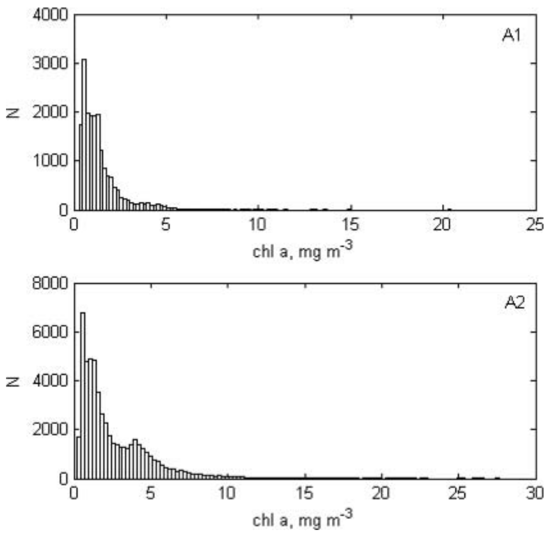

Figure 4. Asymetric distributions of chl *a* in the offshore waters of SYS and its vicinities (A1 and A2) during September 1997 to August 1998. Pixels with value higher than 30 mg m^{-3} were excluded as pixel-mixing noises at land-water zone.

the same time period. Therefore the overall composition (proportion of phytoplankton and non-phytoplankton particles) changed. This change in the particulate assemblage was also depicted by γ that exhibited a significant declining trend for both nearshore waters ($p < 0.01$) and offshore waters ($p < 0.05$) (Figure 6c). This pattern indicates that the relative proportion of large particles tends to increase compared to smaller ones from 1997 to 2007.

Discussion

Nearshore waters are generally associated with greater chl *a* and $b_{bp}(490)$ and lower γ than offshore waters. This is in good agreement with expectations, as coastal areas are generally more productive and the relatively high content of phytoplankton can increase the number of larger particles in nearshore waters. This spatial distribution pattern of γ may be partly attributable to the spatial characteristics of size structure of phytoplankton, as well as to the deposition of particles. In situ work in this area show that the proportion of small-size phytoplankton cells for the offshore waters is larger than for the nearshore waters, and vice versa (Deng et al., 2008); Fu et al. (2009) shows a similar spatial pattern in size-fractionated chl *a*, i.e. the chl *a* of larger-sized phytoplankton (>2 μm) is larger for the nearshore waters than for the offshore waters. The non-algal particles in nearshore waters mainly consist of the sediments from surface runoff and the re-suspended sediments from sea bottom, and larger particles are more likely to settle during the transport from nearshore waters to offshore waters.

A spring phytoplankton bloom occurs in offshore waters of the SYS, but no autumn bloom occurs. In winter, the discharge of river flow decreases to its lowest level (see Figure 7 for the regional land precipitation), and mainly flows southward to the East China Sea rather than toward the SYS due to the prevailing northwesterly wind. Therefore, the winter peak of b_{bp} and chl *a* in the nearshore are

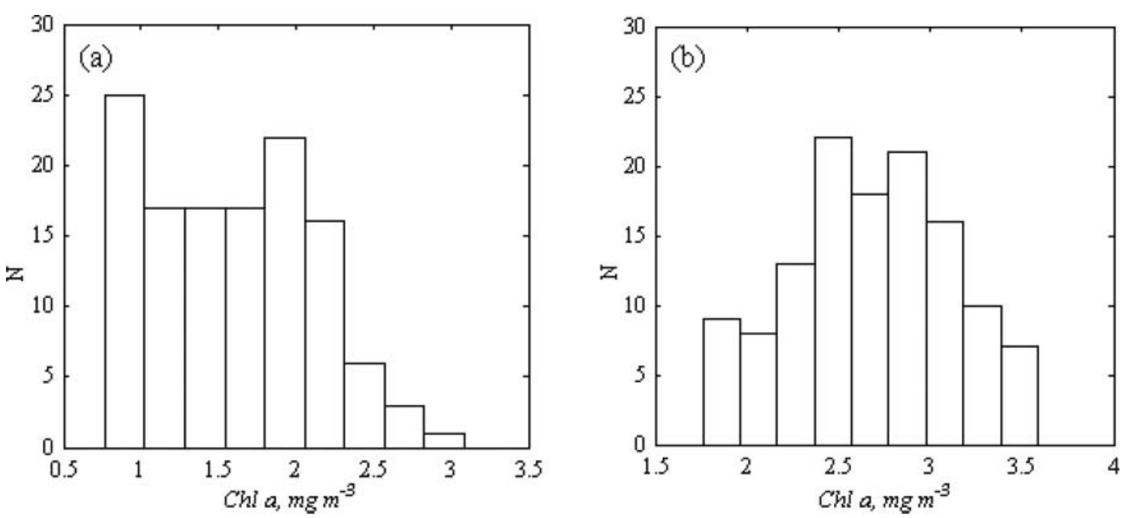

Figure 5. Distributions of spatially-averaged chl *a* in (a) A1 and (b) A2 during the 1997–2007 time period. There is a time series of 120 points in total for each area.

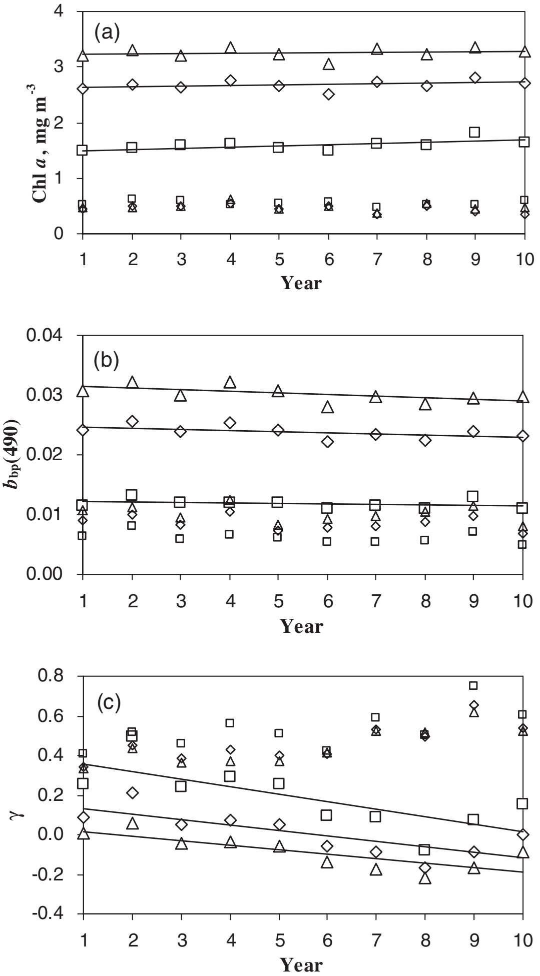

Figure 6. The annual variations of chl *a*, $b_{bp}(490)$ and γ in the Southern Yellow Sea and its vicinities. The symbols of □, ◇ and △ present the annual mean values of each parameter in A1, A2 and A3, respectively, and the smaller ones correspond to their standard deviations.

not due to river inputs, but may be due to wind-driven resuspension. Limiting factors such as nutrients, temperature, light conditions, and phytoplankton species may help to explain the difference (Yang et al., 2004). This finding may help to improve the ecological modeling in the Yellow Sea (Hu et al., 2004).

The observed increase in chl *a* for the offshore waters of SYS during the time period 1997–2007 is not accompanied by a similar trend in $b_{bp}(490)$. No significant trend is observed for $b_{bp}(490)$, which implies that the whole particulate pool seen by b_{bp} does not significantly change in concentration, but may change in composition. According to these

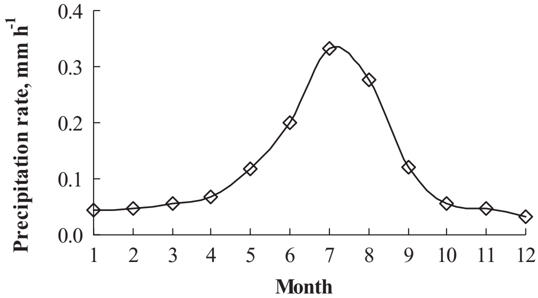

Figure 7. The seasonal patterns of precipitation over the land at the west of SYS. The data of precipitation rate were retrieved from the satellite sensors of TMI, QuikScat; for more details about the data, one can refer to the NASA's website.

results one may expect that the non-algal particulate pool concentration should decrease between 1997 and 2007. The declining trend in γ is in agreement with that of chl *a*, which is consistent with recent observations performed over the global ocean (Vantrepotte et al., 2011). If it is assumed that the suspended sediments, the major non-algal particles in this region, have no significant inter-annual changes in size distribution, then the changes of γ are mainly dominated by the phytoplankton particles. The lower value of γ indicates a greater proportion of larger-size phytoplankton in particle assemblages. A greater proportion of larger-size phytoplankton is usually linked to higher chl *a* concentration. So, the declining trend in γ provides evidence for the increase in phytoplankton biomass. A decreasing trend in chl *a* observed for the middle and low-latitude oceans from 1998 to 2006, has been attributed to El Niño/Southern Oscillation (ENSO) at the low-latitude zone of global open oceans (Behrenfeld et al., 2006). Unlike the global open oceans, the phenomenon at the SYS is most likely related to local eutrophication (Yoo et al., 2010).

There are many factors which may influence the ecosystem of the SYS, e.g. the runoff from the coastal small rivers, coastal urban sewage, the wastewater of aquaculture, wind-induced turbulence, and even the Kuroshio Current. The Yangtze River is the biggest river close to the SYS, but it seems that the river has no pronounced impacts on chl *a* especially at the offshore waters of SYS. Since the completion of the Three Gorges Dam in 2003, water and sediment discharges have decreased (Yang et al., 2006), and a decrease in nutrient loading was also expected. However, chl *a* in the central SYS increased during this period. The low value of chl *a* in Summer and Autumn (Figure 2) occurs at the time of peak flux of water and nutrients during the wet season (Summer–Autumn) of the Yangtze River watershed. For the nearshore, the winter bloom is not likely caused by river input during the dry season, but the autumn bloom is consistent with river discharge in wet season (Figure 2).

Conclusions

As detected by the remotely sensed data of chl *a*, the waters in the South Yellow Sea showed an increasing trend in phytoplankton biomass during the time period 1997–2007, and there was a significant increase rate of about 0.02 mg m^{-3} y^{-1} in chl *a*. A significant inter-annual change in the spectral slope of the particulate backscattering coefficient, γ, suggests an increasing trend of the proportion of larger-particles–phytoplankton in the particle assemblages. This trend is opposite of the declining trend of phytoplankton biomass in global middle- and low-latitude waters. We think that the chlorophyll increase in the SYS is mostly driven by localized environmental changes, i.e. eutrophication caused by higher nutrient inputs from land.

Two different seasonal patterns of phytoplankton were also observed in the SYS waters: nearshore waters are characterized by the occurrence of two chl *a* peaks: one in spring (February), the other in autumn (August). In contrast, offshore waters of the central SYS are characterized by only one spring bloom peak in April. These findings may help in the understanding of the dynamics of the local aquatic ecosystem and improve its modeling.

Acknowledgements

This work was supported by the project from CAS, China (No. KZCX2-YW-Q07–01) and the CAS/SAFEA International Partnership Program for Creative Research Teams–"Representative environmental processes and resources effects in coastal zone" by CNRS (France) through a postdoctoral fellowship and CNES (France) through the COULCOT project in the frame of the TOSCA program. We are grateful to NASA Goddard Space Flight Center (GSFC) for providing the SeaWiFS ocean color data (http://oceancolor.gsfc.nasa.gov/). The valuable comments on our work from two anonymous reviewers are also highly appreciated.

References

Behrenfeld, M., O'Malley, R., Siegel, D., McClain, C., Sarmiento, J., Feldman, G., Milligan, A., Falkowski, P., Letelier, R., Boss, E., 2006. Climate-driven trends in contemporary ocean productivity, Nature, 444, 752–755. doi:10.1038/nature05317.

Carder, K. L., Chen, F. R., Lee, Z. P., Hawes, S., Kamykowski, D., 1999. Semi-analytic MODIS algorithms for chlorophyll a and absorption with bio-optical domains based on nitrate-depletion temperatures, J. Geophys. Res. 104(C3), 5403–5421.

Chen, B., Chen, J., Cui, Y., Li, Q., Yuan, Y., 2001. The ecological characteristics of phytoplankton in the eastern marineculture area of Laizhou Bay. Marine Fisheries Research, 22(3), 64–70.

Deng, C., Yu, Z., Yao, P., Chen, H., Xue, C., 2008. Size-fractionated phytoplankton in the East China and Southern Yellow Seas and its environmental factors in Autumn 2000, Period. Ocean Univ. China, 38 (5), 791–798.

D'Sa, E. J., Miller, R. L., McKee, B. A., 2007. Suspended particulate matter dynamics in coastal waters from ocean color: Application to the northern Gulf of Mexico, Geophys. Res. Lett. 34, L23611, doi:10.1029/2007GL031192.

Fu, M., Wang, Z., Li, Y., Li, R., Sun, P., Wei, X., Lin, X., Guo, J., 2009. Phytoplankton biomass size structure and its regulation in the Southern Yellow Sea (China): Seasonal variability. Continental Shelf Research, 29, 2178–2194.

Hu, H., Wan, Z., Yuan, Y., 2004. Simulation of seasonal variation of phytoplankton in the southern Huanghai (Yellow) Sea and analysis on its influential factors, Acta Oceanol. Sin., 26(6), 74–88.

Kopelevich, O. V., 1983. Small-parameter model of optical properties of sea water. In: A. S. Monin (Eds.), *Ocean Optices, Chapter 8, Vol. 1*. Nauka Pub., Moscow, Russian.

Kostadinov, T.S., Siegel, D.A., Maritorena, S., Guillocheau, N., 2007. Ocean color observations and modeling for an optically complex site: Santa Barbara Channel, California, USA, J. Geophys. Res. 112, C07011, doi: 10.1029/2006JC003526

Li, C., Zhang, F., Shen, X., Yang, B., Shen, Z., Sun, S., 2005. Concentration, distribution and annual fluctuation of chlorophyll-*a* in the Jiaozhou bay, Oceanol. Limnol. Sin. 36(6), 499–506.

Liu, D. Y., Keesing, J. K., Xing, Q. G., Shi, P., 2009. World's largest macroalgal bloom caused by expansion of seaweed aquaculture in China, Mar. Pollut. Bull., doi:10.1016/j.marpolbul.2009.01.013.

Loisel, H., Stramski, D., 2000. Estimation of the inherent optical properties of natural waters from irradiance attenuation coefficient and reflectance in the presence of Raman scattering. Applied Optics. 39, 3001–3011.

Loisel, H., Nicolas, J. M., Sciandra, A., Stramski, D., Poteau, A., 2006. Spectral dependency of optical backscattering by marine particles from satellite remote sensing of the global ocean, J. Geophys. Res. 111, C09024, doi:10.1029/2005JC003367.

Loisel, H., Lubac, B., Dessailly, D., Duforêt-Gaurier, L., Vantrepotte, V., 2010. Effect of inherent optical properties variability on the chlorophyll retrieval from ocean color remote sensing: an in situ approach. Optics Express, Vol. 18, No. 20.

McClain, C.R., 2009. A decade of satellite ocean color observations. Annual Review of Marine Science 1, 19–42.

Mobley, C. D., 1994. *Radiative Transfer in Natural Waters. In light and water.* Academic Press, San Diego.

O'Reilly, J.E., Maritorena, S., Mitchell, B.G., Siegel, D.A., Carder, K.L.,Garver, S.A., Kahru, M., McClain, C., 1998. Ocean color chlorophyll algorithms for SeaWiFS. J. Geophys. Res. 103, 24937–24953.

Reynolds, R. A., Stramski, D., Mitchell, B.G., 2001. A chlorophyll dependent semianalytical reflectance model derived from field measurements of absorption and backscattering coefficients within the Southern Ocean. J. Geophys. Res. 106, 7125–7138.

Vantrepotte, V., Loisel, H., F. Mélin, F., Dessailly, D., Duforêt-Gaurier, L., 2011. Global particulate matter pool temporal variability over the SeaWiFS period (1997–2007). Geophys. Res. L., Vol. 38 L02605, doi:10.1029/2010GL046167

Wozniak, S. B., Stramski, D., 2004. Modeling the optical properties ofmineral particles suspended in seawater and their influence on ocean reflectance and chlorophyll estimation from remote sensing algorithms, Appl. Opt. 43, 3489–3503.

Yang, D. F., Gao, Z. H., Chen, Y., Wang, P. G., Sun, P. Y., 2004. Influence of seawater temperature on phytoplankton growth in Jiaozhou Bay, China. Chinese Journal of Oceanology and Limnology, 22(2), 166–175, DOI: 10.1007/BF02842589.

Yang, Z., Wang, H., Saito, Y., Milliman, J. D., Xu, K., Qiao, S., Shi, G., 2006. Dam impacts on the Changjiang (Yangtze) River sediment discharge to the sea: The past 55 years and after the Three Gorges Dam, Water Resour. Res. 42, W04407, doi:10.1029/2005WR003970.

Yoo, S., An, Y.-R., Bae, S., Choi, S., Ishizaka, J., Kang, Y.-S., Kim, Z.G., Lee, C., Lee, J.B., Li, R., Park, J., Wang, Z., Wen, Q., Yang, E. J.,Yeh, S.-W., Yeon, I., Yoon, W.-D., Zhang, C.-I., Zhang, X., Zhu, M., 2010. Status and trends in the Yellow Sea and East China Sea region, In: S.M. McKinnell and M.J. Dagg (Eds.), *Marine Ecosystems of the North Pacific Ocean, 2003–2008*. pp. 360–393. PICES Special Publication, http://www.pices.int.